

# DESIGN AND EXPERIMENTAL ANALYSIS OF ROTARY SPOON SOYBEAN PRECISION SEEDER

## 转勺式大豆精密排种器设计与试验分析

Qichao LI<sup>1)</sup>, Jinlong FENG<sup>1\*)</sup>

<sup>1)</sup> College of Mechanical and Electrical, Lingnan Normal University, Zhanjiang 524048, China

\*Corresponding authors, Email: qc\_lee@126.com

DOI: <https://doi.org/10.35633/inmateh-74-01>

**Keywords:** soybean; precision sowing; rotary spoon style; seeder; fastest descent line

### ABSTRACT

To optimize the structure of soybean precision seeder and improve the performance of sowing, a new rotary spoon precision seeder is designed, and the key component structure is designed using numerical calculation methods. Using a combination of bench experiments and field experiments for parameter optimization experiments, a multi factor quadratic orthogonal rotation combination design experiment is adopted. The experimental data is analyzed and processed using Design Expert 8.0.6 software to seek the optimal combination of parameters. The results show that when the working speed is 24.56 ~ 33.72 r/min and the forward speed is in the range of 1.31 ~ 2.21 m/s, the seeding qualification index is greater than 90% and the coefficient of variation is less than 10%, meeting the requirements of excellent seeding standards. This study uses a rotary spoon seeder to sow soybeans, providing a new idea and reference for the development of precision soybean seeders.

### 摘要

为优化设计大豆精密排种器结构, 提高播种作业性能, 设计一种新型转勺式精密排种器, 采用数值计算方法设计关键部件结构。通过台架试验与田间试验相结合的方法进行参数优选试验, 设计试验采用多因素二次正交旋转组合方法, 运用 Design Expert 8.0.6 软件分析处理试验数据, 寻求最优作业参数组合。结果表明: 工作转速 24.56~33.72 r/min, 前进速度 1.31~2.21 m/s 范围时, 播种合格指数>90%, 变异系数<10%, 达到播种优等标准要求。该研究利用转勺式排种器播种大豆, 为大豆精密排种器的研发提供了创新思路和借鉴参考。

### INTRODUCTION

Soybean, as an important grain and oil crop, has been continuously expanded in planting scale, and the demand for precise sowing is increasing day by day. Precision sowing machinery is used to accurately and quantitatively sow seeds into predetermined positions in the soil, ensuring uniform three-dimensional spatial distribution between seeds. The core component of a soybean seeder is the seeder, whose structure and working principle determine the quality of sowing and directly affect soybean yield (Dayoub et al., 2021; Badua et al., 2021; Sharma et al., 2024; Noureldin et al., 2019; Wang et al., 2021; Šarauskiis et al., 2023). The main types of soybean seeders are mechanical and air suction. Air suction is applied due to its light damage to seeds and relaxed requirements for seed shapes, which is conducive to high-speed sowing by large machinery. However, its complex structure, high price, and high-power requirements are not conducive to the application of small machinery. Mechanical seeders have been widely used due to their simple structure, low cost, and strong applicability (Akhalaia et al., 2021; Baghoee et al., 2023; Chen et al., 2020; Akhalaya et al., 2021).

Many studies have been conducted on mechanical soybean seeders. Emrah et al (2021) designed a slotted wheel seeder device. Through optimizing the design of the slotted wheel, the damage to the seeder was reduced, and the lowest crushing rate was achieved at a forward speed of 2 m/s. Kumar et al (2017) designed a disc seeding device to overcome seed damage, seed loss, and uneven seed distribution. Laryushin et al (2021) designed a disc groove seeding device, in which the filling groove of the cross-section is designed as a ring shape to improve the uniformity of seeding. Kokuryu (2021) developed a slanted hole disc seeder that can supply seeds on both sides and is used for large-scale high-speed sowing. Hensh and Raheman (2022) designed an electromagnetic driven seeder that driven by a push-pull solenoid valve. The seeds are transported through a rectangular hole wheel disc and thrown out at the outlet to improve seeding accuracy.

---

Qichao LI, Associate professor, Ph.D.; Jinlong FENG, Lecturer, Ph.D.

Zhang *et al* (2022) optimized the height difference design of the hole edge at the filling end of the disc soybean seeder to reduce the overhead problem of soybean seeds during the filling process. Huang *et al* (2022) designed a side mounted guided soybean precision seeder with a hole structure that facilitates the shape of seed filling, solving the problem of poor seed filling effect of existing mechanical seeders during high-speed operations. Li *et al* (2024) designed a dual row seed disc-shaped hole staggered distributed seed planter. The independent dual cavity structure reduces the speed of the seeder and avoids the population accumulation and mutual interference affecting seed filling. The above studies mainly focus on improving the hole structure of the sowing, increasing sowing accuracy or reducing damage rate. However, these studies only focus on innovative optimization of the hole structure of the wheel sowing device, and there is relatively little researches and applications of the spoon soybean sowing device.

In response to the limitations of the above researches, to improve the operational quality of mechanical soybean precision seeders, a rotary spoon soybean precision seeder is designed. Its structure and working principle are analyzed, and the key component structural parameters are optimized. The multi factor quadratic orthogonal rotation combination experimental method is used to optimize the seeding and parameters of the seeder, providing theoretical support and innovative ideas for the development of precision soybean seeding.

## MATERIALS AND METHODS

### Structure and Working Principle of the Seeder

The overall structure of the seeder mainly consists of an upper cover, dual drive disc (cam groove limit track disc, drive turntable, seed spoon base), seed spoon, seed guide tube, seed container, seed storage box and other components, as shown in Fig. 1 (a). The seed spoon and dual drive disc are the core components, and their reasonable configuration can smoothly complete the tasks of seed filling, seed holding, and seed feeding. The structure of the seed spoon is a near spherical crown, which can reduce the probability of seed slipping and damage during seed picking, and improve seed adaptability. The other end is directly connected to the base installed on the drive turntable, and the tail end of the base is embedded in the grooves of the cam groove limit track disc. The design of the upper mouth of the seed guide tube is lengthened to increase the feeding stroke and improve the effective seeding. The side wall is provided with an open seed partition plate, which is in contact with the seed shell. The seed shell is divided into two parts: the seed filling area and the seed storage area. The seeds in the seed storage area can flow into the seed filling area through the opening, and the whole is closed by the upper cover. The final assembly drawing is shown in Fig. 1 (b).

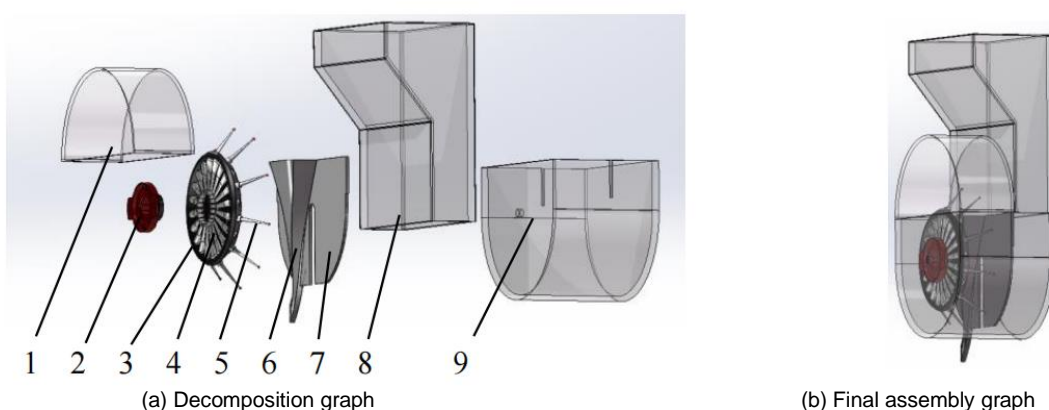


**Fig. 1 - Structure of the seeder**

1. Upper cover; 2. Cam groove limit track disc; 3. Drive turntable; 4. Base; 5. Seed spoon; 6. Seed guide tube; 7. Seed separator; 8. Seed storage box; 9. Seed container

The working process of the seeder is mainly divided into three stages: seed filling, seed holding, and seed feeding. During operation, the seeds in the seed storage box flow into the seed filling area under the action of gravity. The number of seeds flowing into the seed filling area is controlled by the seed container and the seed separator, ensuring that the number of seeds in the seed filling area is sufficient and in dynamic balance. The driving turntable drives the seed spoon and the base to rotate steadily in the circumferential direction. The tail end of the base is located in the grooves of the cam groove limit track disc. Under the joint action of the driving turntable and the cam groove limit track disc, the seed spoon and the base rotate regularly to ensure effective seed filling, stable seed holding, and precise seed feeding of the seed spoon.

When filling seeds, the seeds are divided under the rotation and agitation of the seed spoon, forming a population layer with different speeds. The seed filling process is completed under the combined action of its gravity, centrifugal force, collision friction between populations, and the force of the seed spoon. During the seed holding stage, the spoon slightly tilts upwards to ensure that a single seed does not fall off during rotation, achieving a smooth seed holding. When the seeds are transported to the sowing area, the spoon mouth flips downwards due to the rotation of the seed scoop. The seeds are precisely thrown into the seed guide tube under their gravity and centrifugal force, completing the sowing process.

### Structural design of seed spoon

The seeding spoon is one of the key components of the spoon seeding device, and its structural shape, size parameters, and arrangement directly affect the seeding and feeding of the seeding device. Therefore, it is required that the seed scoop scoops the seeds and rotates them in all directions smoothly without falling off, and the seeds slide smoothly without obstacles when drop. 1000 soybean seeds (Zhonglong 3) are selected randomly for three-axis size measurement, and the average values are respectively  $l = 5.3 \text{ mm}$ ,  $w = 5.0 \text{ mm}$ ,  $h = 4.9 \text{ mm}$  as approximately spherical.

The formula for calculating the projected cross-sectional area is as follows:

$$\begin{cases} S_h = \pi lw \\ S_w = \pi lh \\ S_l = \pi wh \end{cases} \quad (1)$$

where,  $S_h$ —The projected cross-sectional area when the seeds are in a supine state,  $\text{mm}^2$

$S_w$ —The projected cross-sectional area when the seeds are in a side-standing state,  $\text{mm}^2$

$S_l$ —The projected cross-sectional area when the seeds are in an upright state,  $\text{mm}^2$

During the process of filling seeds with a seed spoon, the probability of the posture distribution of seeds scooped into the spoon under the action of gravity and friction is positively correlated with the projected cross-sectional area (Zhang, 1997), and it is an incompatible event.

The calculation formula is as follows:

$$P_h + P_w + P_l = 1 \quad (2)$$

$$\begin{cases} P_h = \frac{S_h}{S_h + S_w + S_l} \times 100\% \\ P_w = \frac{S_w}{S_h + S_w + S_l} \times 100\% \\ P_l = \frac{S_l}{S_h + S_w + S_l} \times 100\% \end{cases} \quad (3)$$

Where:

$P_h$ —Probability of distribution in a supine position, %

$P_w$ —Probability of distribution in a side-standing position, %

$P_l$ —Probability of distribution in an upright position, %

According to Eqs. (2) and (3), the probabilities of seeds being placed in three positions of supine, side-standing, and upright in the seed spoon are calculated to be 34.4%, 33.8%, and 31.8%, respectively. Based on the geometric parameters of seeds and the probability of attitude distribution, combined with the principle of the steepest descent curve, the internal structure of the seed scoop is simplified. The solid of the seed scoop is optimized as a near spherical crown by rotating and scanning the curve, as shown in Fig. 2. The main structural parameters are the spoon mouth diameter  $D$ , the spoon depth  $H$ , and scanning curve parameters, and the design should follow principles  $D > l > w > h > H > 0.7l$  (Gulati and Singi, 2003).

Based on the measurement of the three-axis size parameters of the seeds, a seed scoop is designed with an opening diameter of  $D = 5.5 \text{ mm}$  and a depth of  $H = 4.0 \text{ mm}$ .

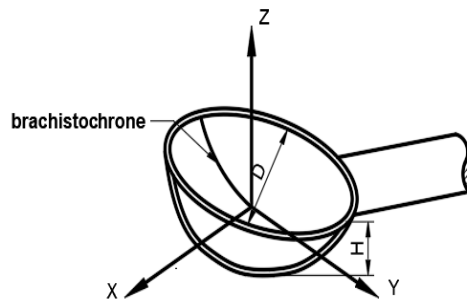


Fig. 2 - Seed spoon

When the seed rolls from the mouth to the bottom of the spoon, the shortest time path it experiences is the steepest descent curve. The particle *M* rolling from the starting point *O* to the non-directly below endpoint *K* is the curve with the shortest time, as shown in Fig. 3. The rolling circle with radius *r* rolls along the straight-line *OB*, and the trajectory swept by a point *M* on the edge of the circle is the steepest descent line between points *O* and *K*.  $\theta$  is the angle of rotation, *r* is the radius of curvature, and the equation for the trajectory of the steepest descent line is (Akhshik et al., 2015) as follows:

$$\begin{cases} x = r(\theta - \sin \theta) \\ z = r(1 - \cos \theta) \end{cases} \quad \theta \in [0, \pi / 2] \quad (4)$$

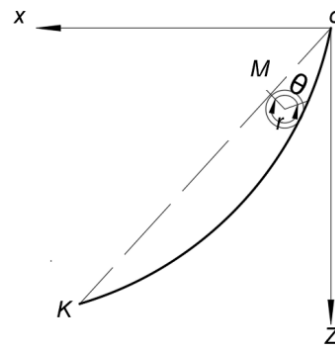


Fig. 3 - The principle of the steepest descent line

The abstract model schematic diagram based on the actual movement of the seed filling and scooping spoon is shown in Fig. 4. Using the center of the bottom of the seed spoon as the coordinate origin *o*, a spatial Cartesian coordinate system *o-vyz* is established to study the motion state of seeds in the *xoz* plane, then

$$\begin{cases} mg \cos \beta = F_N \\ F_s = F_N \tan \varphi \end{cases} \quad (5)$$

- where *m* - the quality of a single seed, (g);
- g* - gravitational acceleration, (m/s<sup>2</sup>);
- $\beta$  - the tangent inclination angle of the truncated curve at the sliding point, (°);
- $\varphi$  - the friction angle between seed and spoon, (°);
- F<sub>N</sub>* - the support of the spoon on seeds, (N);
- F<sub>s</sub>* - the friction force of spoon on seeds, (N).

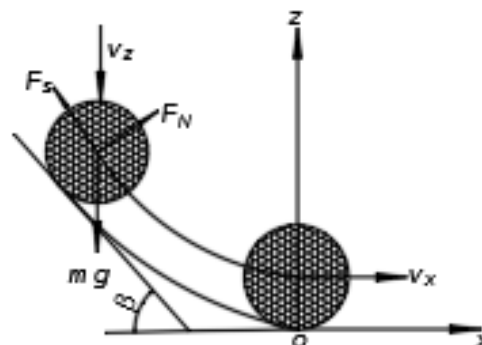


Fig. 4 - The cut-through curve of the fastest descent line

During the seed filling process, when the height of the seed rolling is  $h$  (the maximum value is the hole depth  $H$ ), its lateral displacement is  $\frac{\theta - \sin \theta}{1 - \cos \theta} h$ . The work done by the frictional force  $F_s$  when the seed rolls down along the steepest descent line to the bottom of the spoon is as follows:

$$\int_0^{\frac{\theta - \sin \theta}{1 - \cos \theta} h} mg \cos \beta \tan \varphi dx = mgh \cos \beta \tan \varphi \frac{\theta - \sin \theta}{1 - \cos \theta} \quad (6)$$

According to the law of conservation of energy, that is:

$$\frac{1}{2} m(v_z^2 - v_x^2) + mgh = mgh \cos \beta \tan \varphi \frac{\theta - \sin \theta}{1 - \cos \theta} \quad (7)$$

where  $v_z$  - the initial descent speed of seeds, (m/s);

$v_x$  - the seed termination horizontal speed, (m/s);

Combining and simplifying Eqs. (4) to (7), it can be obtained:

$$z = \frac{2gh \cos \beta \tan \varphi}{v_z^2 - v_x^2 + 2gh} x \quad (8)$$

From this, it can be concluded that the tangent inclination angle  $\beta$  is:

$$\beta = \arcsin \left[ \sqrt{1 + \left( \frac{v_z^2 - v_x^2 + 2gh}{2gh \tan \varphi} \right)^2} - \frac{v_z^2 - v_x^2 + 2gh}{2gh \tan \varphi} \right] \quad (9)$$

The friction angle between the seed and the spoon is  $\varphi = 33 \sim 43^\circ$ . In an ideal state, the initial velocity of the seed is  $v_z = 0$  m/s, and the velocity of rolling to the bottom of the spoon is  $v_x = 0$  m/s. Substituting it into Eq. (9), the tangent angle  $\beta$  of the steepest descent curve can be obtained as  $\beta = 30 \sim 37^\circ$ .

**Dual drive wheel design**

The dual drive wheel disc consists of a drive turntable and a cam groove limit track disc, and a seed spoon base is installed on the drive turntable. The cam groove limit track disc is used to restrict the movement trajectory of the spoon base, and its model structure is shown in Fig. 5.

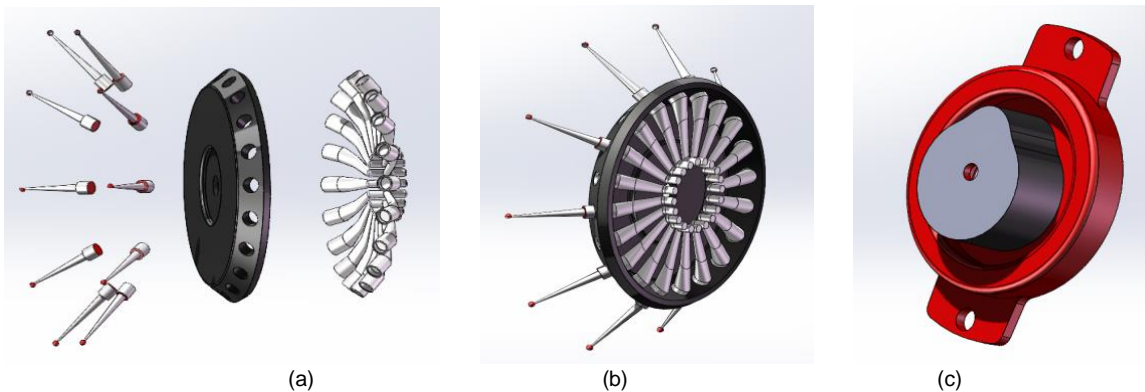


**Fig. 5 - Dual drive disc structure**

(a) Decomposition diagram of drive turntable and base; (b) Assembly diagram of seed spoon and drive turntable  
(c) Cam groove limit track disc

The smooth coordination of the two plates can accurately and timely control the seed spoon to complete the tasks such as filling, holding, and feeding. The principle of dividing the working areas of the seeder should follow: the filling area should be designed as large as possible to ensure sufficient filling time, stable and reliable filling efficiency, and avoid too large filling area that causes seed wear; the seed holding area is the natural sliding of excessive seeds as soon as possible to ensure the smooth transportation of individual seeds to the planting area; the seeding area keeps the seeds thrown accurately and quickly, so as to prevent the spoon and seeds from crossing the seeding area and missing the seeding port. According to this principle, combined with the position of the population in the seeder, the angles of the filling area I, the holding area II, the sowing area III, the empty sowing area IV, are designed to be  $130^\circ$ ,  $90^\circ$ ,  $50^\circ$  and  $90^\circ$ , respectively, as shown in Fig. 6.

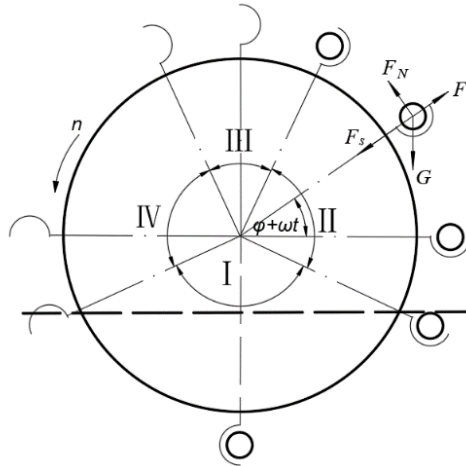


Fig. 6 - Regional division and seed stress analysis

To improve the seeding performance of the seeder, it is required that the force during seed transportation be stable. The critical condition for seeds to be relatively balanced in a spoon and not thrown away is analyzed. A mechanical model is established based on the D'Alembert principle:

$$\begin{cases} mg \sin(\varphi + \omega t) + F_s = F_e \\ F_N = mg \cos(\varphi + \omega t) \\ F_e = mR\omega^2 = 4\pi^2 mRn^2 \\ F_s = \mu F_N \end{cases} \quad (10)$$

where  $m$ —seed quality, (g);

$\mu$ —friction coefficient between seed and spoon wall (0.32~0.43)

$F_e$ —centrifugal force of seeds, (N);

$\omega$ —angular velocity of motion, (rad/s);

$(\varphi + \omega t)$ —rotation angle,  $(0, \pi/2)^\circ$

The second derivative of the radial decomposition in Eq. (8) is obtained as follows:

$$\frac{d^2 F_N}{d\omega^2} = -mgt^2 [\sin(\varphi + \omega t) + \mu \cos(\varphi + \omega t)] - 2mR \quad (11)$$

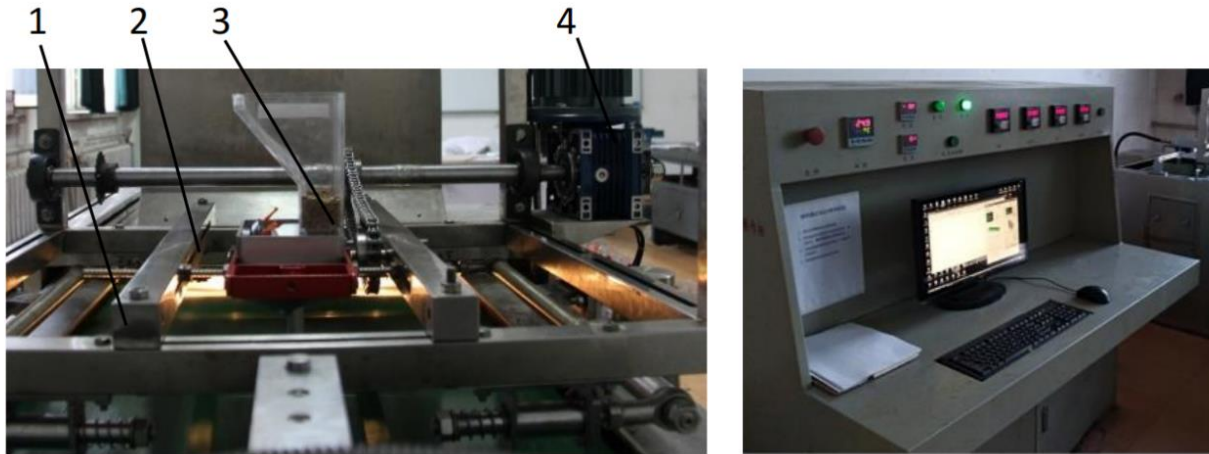
According to the rotation angle range  $(0, \pi/2)$  of the seeding wheel, it can be determined that the second-order derivative of Eq. (11) is always less than zero, that is, the radial force function of the spoon holding seed is changing along the convex curve. Therefore, it can be inferred that as the working speed increases, the radial force on the seed first increases and then decreases. Therefore, the maximum centrifugal force on the seed should be at the inflection point.

To solve for the critical condition of the seed being thrown away, the working speed limit value  $n$  is obtained by organizing Eq. (10) as follows:

$$n \leq \sqrt{\frac{g[\sin(\varphi + \omega t) + \mu \cos(\varphi + \omega t)]}{4\pi^2 R}} \quad (12)$$

The larger the rotation radius of the seeding spoon of the seeder, the more spoons there are, and the lower the speed, the better the seeding. However, if the radius is too large and the spoon handle is too long, the seeding stability will be worse. The diameter of the drive turntable should not be too small, otherwise the number of seed spoons installed will be small, resulting in an increase in speed. Based on this, the radius of the drive turntable is set to 50 mm; the radius of the cam groove limit plate is 46 mm; the rotation radius  $R$  of the spoon is 56 mm; the number of spoons is 10, and the relative rotation angle is  $25 \sim 90^\circ$ . Substituting it into Eq. (12), it is calculated that if the working speed is below 40.37 r/min, the seeds will remain stable and not fly away, which sets the horizontal critical value of the working speed factor for the experiment.

### Experimental materials and equipment



(a) Test bench for the seed planter performance (b) Data acquisition system

**Fig. 7 - Seed performance test bench**

1. Transmission bed belt; 2. Installation rack; 3. Seeder; 4. Motor

The experimental material is soybean (Zhonglong 3), and the experimental location is the Seed Performance Laboratory of Northeast Agricultural University. The experimental equipment includes the JPS-12 computer vision seeder performance testing platform and seeder, as shown in Fig. 7. During the experiment, the seeder is fixed on the test bench and maintained in a horizontal seeding state. The motor controls the speed of the seeder, and another motor controls the speed of the seedbed conveyor belt to simulate the forward state of the seeding machine. The data collection and statistical processing are carried out through the image acquisition and processing system of the test bench, so as to accurately measure different seeding performance indicators.

### Test methods

According to the requirements of soybean growth and agronomic characteristics, combined with the actual sowing conditions in Heilongjiang Province, a single row sowing spacing of 8 cm is set to ensure uniform sowing during the operation. Referring to GB/T6973-2005 "Test methods for single seed drills (precision drills)" and JB/T1029-2001 "Specifications for single seed drills (precision drills)", the seeding qualification index and coefficient of variation are selected as the test indicators to evaluate the performance of the seeder. The calculation formula is as follows:

$$S = \frac{n_1}{N} \times 100\% \quad (13)$$

$$C = \sqrt{\frac{\sum(l - \bar{l})^2}{(N-1)\bar{l}^2}} \times 100\% \quad (14)$$

where  $S$ —qualification index, (%);

$C$ —coefficient of variation, (%);

$n_1$ —number of qualified seeds per grain, (piece);

$N$ —total theoretical seeds of hole spacing, (piece);

$l$ —theoretical sowing distance, (cm);

$\bar{l}$ —average sowing distance, (cm).

### RESULTS AND ANALYSIS

Under the premise of determining the structural parameters of the seeder, the main factors affecting the performance of the seeder are the working speed and forward speed of the seeder. Therefore, two factors are selected as experimental factors, and a two factor five level quadratic regression rotation orthogonal combination design experiment is adopted to seek the optimal working parameter combination of the seeder. The working speed  $v_1$  of the seeder is set in the range of 20 ~ 40 r/min, and the forward speed  $v_2$  is set in the range of 1 ~ 3 m/s. The experimental design scheme and measurement results are shown in Table 1. Design Expert 8.0.6 software is used for analysis, as shown in Table 2.

Table 1

Experimental design and results

Number	Experimental factor		Performance index	
	Working speed $v_1$ / r·min <sup>-1</sup>	Forward speed $v_2$ / m·s <sup>-1</sup>	Qualified index $S$ / %	variable coefficient $C$ / %
1	-1	-1	88.01	11.97
2	+1	-1	81.59	7.67
3	-1	+1	76.08	13.95
4	+1	+1	74.46	11.56
5	-1.414	0	88.09	13.23
6	+1.414	0	79.23	10.65
7	0	-1.414	82.79	9.75
8	0	+1.414	70.16	11.78
9	0	0	90.88	9.22
10	0	0	93.62	8.93
11	0	0	90.67	7.93
12	0	0	89.49	7.34
13	0	0	94.91	6.91
14	0	0	93.67	6.32
15	0	0	92.55	7.67
16	0	0	90.39	8.99

Table 2

Measured test data from variance analysis

Indexes	Sources	Sum of squares	Degree of freedom	Mean square	F	P
Qualified indexes	Models	853.92	5	170.78	59.31	< 0.0001
	$v_1$	52.89	1	52.89	18.37	0.0016
	$v_2$	170.40	1	170.40	59.17	< 0.0001
	$v_1 v_2$	5.76	1	5.76	2.00	0.1876
	$v_1^2$	140.41	1	140.41	48.76	< 0.0001
	$v_2^2$	484.46	1	484.46	168.23	< 0.0001
	Residual	28.80	10	2.88		
	Fitting	2.70	3	0.90	0.24	0.8648
	Error	26.10	7	3.73		
	Sum	882.71	15			
Coefficient of variation	Models	74.73	5	14.95	16.80	0.0001
	$v_1$	13.36	1	13.36	15.02	0.0031
	$v_2$	9.55	1	9.55	10.74	0.0083
	$v_1 v_2$	0.91	1	0.912	1.03	0.3351
	$v_1^2$	33.72	1	33.72	37.91	0.0001
	$v_2^2$	17.18	1	17.18	19.32	0.0013
	Residual	8.89	10	0.89		
	Fitting	2.29	3	0.76	0.81	0.5281
	Error	6.61	7	0.94		
	Sum	83.62	15			

Note: \*\* means extremely significant ( $P < 0.01$ ); \* means significant ( $0.01 < P < 0.05$ ), same as below.

According to the analysis in Table 2, the working speed and forward speed have an extremely significant impact on the sowing qualification index, coefficient of variation performance indicators, respectively. The regression equation is meaningful and the fitting degree is good.

The regression equations for fitting the seeding qualification index and coefficient of variation are as follows:

$$S = 92.02 - 2.57v_1 - 4.62v_2 + 1.2v_1v_2 - 4.19v_1^2 - 7.78v_2^2 \tag{15}$$

$$C = 7.80 - 1.29v_1 - 1.09v_2 - 0.48v_1v_2 + 2.05v_1^2 + 1.47v_2^2 \tag{16}$$

To analyze the relationship between sowing indicators and experimental factors more intuitively, Design Expert 8.0.6 software is used to establish corresponding surfaces between the indicators and the two factors, as shown in Fig. 8.



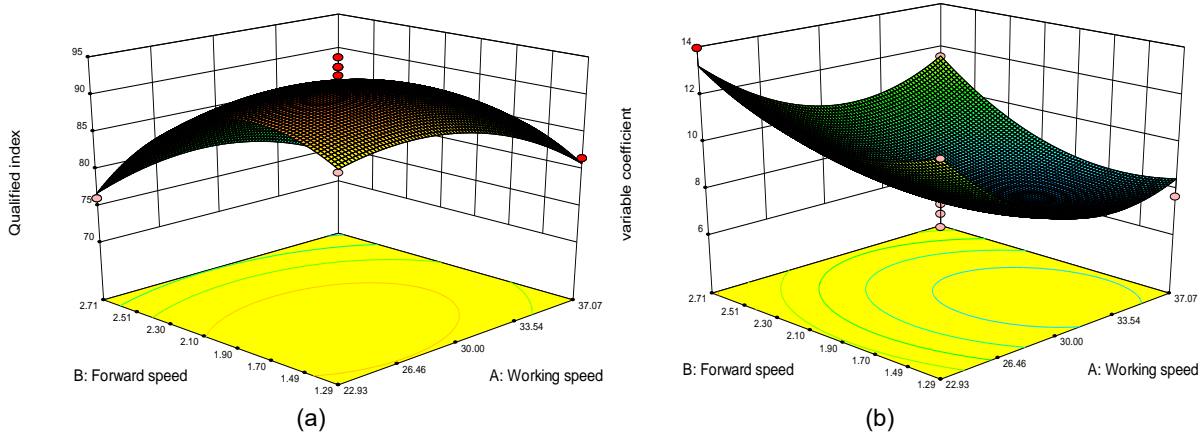


**Fig. 8 - Effects of different working parameters on the indicators**

(a) Effects of working speed and forward speed on the qualified index

(b) Effects of working speed and forward speed on the variable coefficient

According to Eq. (15) and Fig. 8 (a), it can be seen that the qualified index of seed spacing increases first and then decreases with the increase of working speed, and increases first and then decreases with the increase of forward speed. When the working speed is low, the change in the qualification index is gentle, and when it is high, the change increases significantly. When the working speed is around 28 r/min and the forward speed is around 1.8 m/s, the qualification index is the highest.

According to Eq. (16) and Fig. 8 (b), it can be seen that the coefficient of variation decreases first and then increases with the increase of working speed, and decreases first and then increases with the increase of forward speed. When the working speed is low, the coefficient of variation of uniformity changes rapidly, and when it is high, the change is gentle. When the forward speed is low, the coefficient of variation of uniformity changes smoothly, and when it is high, the change is faster. When the working speed is around 37 r/min and the forward speed is around 1.7 m/s, the coefficient of variation is the smallest.

**Optimization of experimental results and parameter combinations**

The optimal combination of working parameters is obtained by analyzing the experimental data, and different factors are optimized for design. According to the agronomic requirements of soybean sowing and combined with boundary conditions of various factors, a parameterized mathematical model is established. Following the requirements of precision sowing, a multi-objective variable optimization method is adopted to analyze the regression equations of sowing qualification index and coefficient of variation.

A nonlinear programming parameter model is established as follows:

$$\begin{cases} \max S \\ \min C \\ s.t. \quad 20r \cdot \text{min}^{-1} \leq v_1 \leq 40r \cdot \text{min}^{-1} \\ \quad 1m / s \leq v_2 \leq 3m / s \\ \quad 90\% \leq S \leq 100\% \\ \quad 0 \leq C \leq 10\% \end{cases} \tag{17}$$

According to the optimization principle, Design Expert 8.0.6 is used for optimization analysis. It is found that when the working speed is 29.47 r/min and the forward speed of the machine is 1.78 m/s, the seeding of the seeder is optimal, with a qualified index of 92.90% for grain spacing and a coefficient of variation of 7.83%. According to the optimization analysis, the optimal parameter combination interval is shown in Fig. 9, that is, when the working speed is between 24.56 ~ 33.72 r/min and the forward speed is in the range of 1.31 ~ 2.21 m/s, the qualified index of sowing distance is greater than 90%, and the coefficient of variation of uniformity is less than 10%.

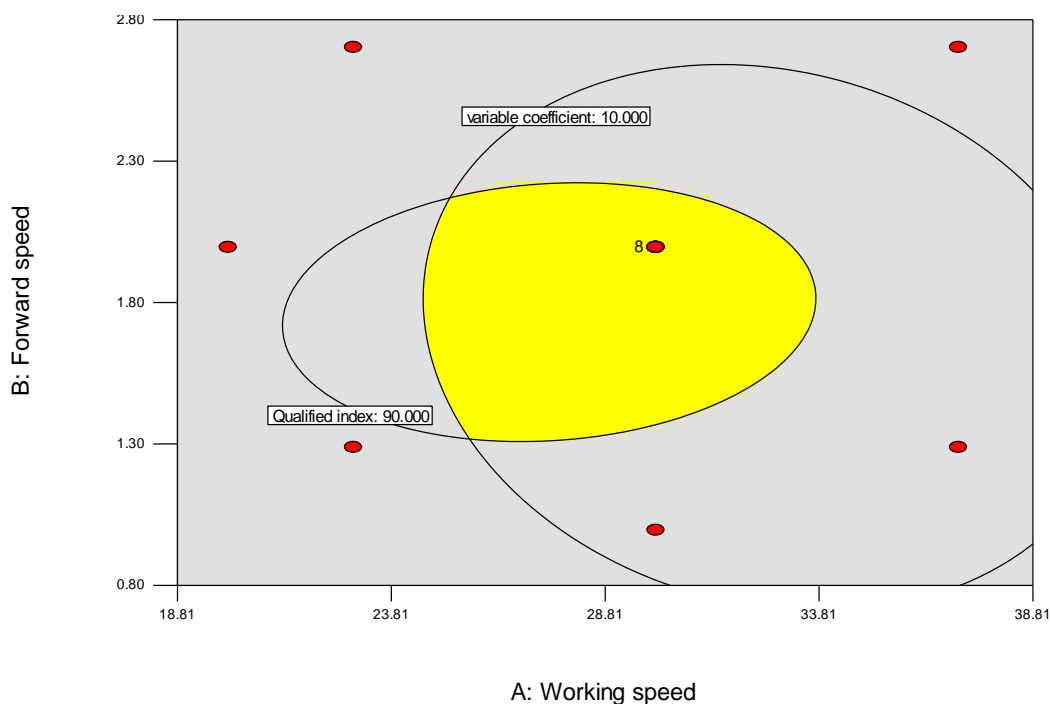


Fig. 9 - Parameters analysis

**Field performance test**

The field sowing performance test was conducted from June to July 2024 at the experimental base of Northeast Agricultural University. Before the experiment, soil was prepared and the soil moisture content was tested to be 17.8 %, with a solidity of  $1.42 \times 10^6$  Pa, which meets the requirements of sowing agriculture. Based on the optimal parameter interval combination optimized by the bench performance test analysis, three sets of data were selected for the experiment. Each set of experimental data was tested three times and the average value was taken. The experimental process is shown in Fig. 10, and the results are shown in Table 3.

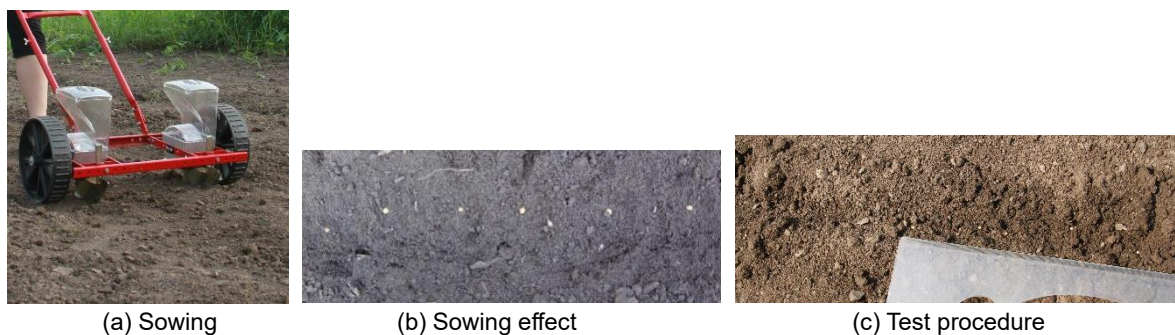


Fig. 10 - Field experiment

Table 3

Results of verification experiment				
Number	Working speed $v_1 / r \cdot \text{min}^{-1}$	Forward speed $v_2 / \text{m} \cdot \text{s}^{-1}$	Qualified index S / %	Variation coefficient C / %
1	26	1.5	91.81	9.12
2	29	1.8	92.92	8.16
3	32	2.1	90.69	9.46

According to Table 3, when the working speed of the seeder is 29 r/min and the forward speed is 1.8 m/s, the combination of the two factors is optimal. When the seeding qualification index is 92.92% and the coefficient of variation is 8.16%, the seeding is optimal. In addition, two sets of parameter combination experiments show that the sowing qualification index is greater than 90% and the coefficient of variation is less than 10%. The experimental results are basically consistent with the theoretical optimization results, meeting the requirements of optimal sowing standards.

## CONCLUSIONS

(1) Based on the physical characteristics of soybean seeds, a seeder is designed. Its structure and working principle are analyzed, and the structural parameters of key components such as the seed spoon, drive turntable, and cam groove limit track are designed.

(2) The bench test investigates the optimal parameter combination of the working speed and forward speed of the seeder, so as to establish a mathematical model between the seeder indicators and experimental parameters. Design Expert software is used for analysis. When the working speed is 29.47 r/min and the forward speed is 1.78 m/s, it is an optimal condition, with a qualification index of 92.90% and a coefficient of variation of 7.83%. Optimizing the regression mathematical model, it is found that when the working speed is 24.5 ~ 33.72 r/min and the forward speed is in the range of 1.31 ~ 2.21 m/s, the qualified index of sowing distance is greater than 90%, and the coefficient of variation of uniformity is less than 10%. This meets the requirements of optimal sowing standards.

(3) Three sets of parameter combinations in the optimized parameter range are selected for field sowing test. When the working speed is 29 r/min and the forward speed is 1.8 m/s, the parameter combination is optimal, with a qualification index of 92.92% and a coefficient of variation of 8.16%, indicating the best seeding. The qualification index of the remaining two evaluation indicators is greater than 90%, and the coefficient of variation is less than 10%. The experimental results are consistent with the optimized model results.

## ACKNOWLEDGEMENTS

Thanks to the Innovation team of intelligence and key technology research for agricultural machinery and equipment in Western of Guangdong province (Grant No. 2020KCXTD039), Horizontal project of intelligent seeder (Grant No. 23060351600030), University Special talent projects (Grant No. ZL22023).

## REFERENCES

- [1] Akhalaia, B.K., Tsench, Y.S., Mironova, A.V. (2021). Development and Research of a Pneumatic Seed Drill Seed Metering unit. *Tekhnika i oborudovanie dlya sela (Техника и оборудование для села)*, Vol. 6, pp. 8-11. <http://dx.doi.org/10.33267/2072-9642-2021-6-8-11>
- [2] Akhalaya, B.K., Shogenov. Y.K., Starovoitov. S.I. (2021). Effect of Design Changes in Pneumatic Seeding Devices on Quality Indicators of Seeding. *Russian Agricultural Sciences*, Vol. 47, pp. 93-98. <https://doi.org/10.3103/S106836742101002X>
- [3] Akhshik, S., Behzad, M., Rajabi, M. (2015). CFD-DEM approach to investigate the effect of drill pipe rotation on cuttings transport behavior. *Journal of Petroleum Science and Engineering*, Vol. 127, pp. 229–244. <http://dx.doi.org/10.1016/j.petrol.2015.01.017>
- [4] Badua, S. A., Sharda, A., Strasser, R., Ciampitti. I. (2021). Ground speed and planter downforce influence on corn seed spacing and depth. *Precision Agriculture*, Vol. 22, pp. 1154-1170. <https://doi.org/10.1007/s11119-020-09775-7>
- [5] Baghooee, M., Karparvarfard, S.H., Azimi-Nejadian, H., Keramat-Jahromi, M., Balanian, H., Sardarpour, F. (2023). DEM Simulation for Seeding Performance of a Slotted Roller Seed-Metering Device for Planting Maize in Laboratory Condition. *Journal of Biosystems Engineering*, Vol. 48, pp. 428-436. <https://doi.org/10.1007/s42853-023-00202-z>
- [6] Chen, W., Zhang, B., Jiang, L., Qiu, T., Wang, L., Yang, S. (2020). Research status and development trend of seed-metering device in China. *American Journal of Agricultural Research*, Vol. 5(11), pp. 98-109. DOI: 10.28933/ajar-2020-06-3006
- [7] Dayoub, E., Lamichhane, J.R., Schoving, C., Debaeke, P., Maury, P. (2021). Early-Stage Phenotyping of Root Traits Provides Insights into the Drought Tolerance Level of Soybean Cultivars. *Agronomy*, Vol. 11(1): 188, <https://doi.org/10.3390/agronomy11010188>
- [8] Emrah, K., Yildiran, Y. (2021). Laboratory Scale of Seed Damage of Coarse-Grain Depending on Groove Diameter and Depth in Roller Devices. *Applied Engineering in Agriculture*, Vol. 37(3), pp. 411-416. <https://doi.org/10.13031/aea.14484>

- [9] Gulati, S., Singi, M. (2003). Design and development of a manually drawn cup type potato planter. *Indian Potato Assoc*, Vol. 30(1), pp. 61-62. India
- [10] Hensh, S., Raheman, H. (2022). Laboratory Evaluation of a Solenoid-Operated Hill Dropping Seed Metering Mechanism for Pre-germinated Paddy Seeds. *Journal of Biosystems Engineering*, Vol. 47, pp. 1-12, <https://doi.org/10.1007/s42853-021-00124-8>
- [11] Huang, Y., Li, P., Dong, J., Chen, X., Zhang, S., Liu, Y. (2022). Design and experiment of side-mounted guided high speed precision seed metering device for soybean (大豆高速播种机侧置导引式精量排种器设计与试验). *Transactions of the Chinese Society for Agricultural Machinery*, Vol. 53(10), pp. 44-53, 75. (in Chinese)
- [12] Kokuryu, T. (2011). High-Speed Seeding with an Inclined-plate Soybean Seeder: Development of the Inclined Cell Plate. *Japanese Journal of Farm Work Research*, Vol. 46(3), pp.107-114. Japan
- [13] Kumar, D., Tripathi, A., Kant, K., Devi, P., Prakash, V. (2017). Design and laboratory test of a seed metering device of sowing soyabean seeds. *Asian Journal of Multidimensional research*. Vol. 6(2), pp. 57-66. India
- [14] Laryushin, N.P., Shukov, A.V., Abakumov, A.V. (2021). Laboratory studies of the sowing unit with the grooves of the coil made in the shape of a torus. *The Agrarian Scientific Journal (Аграрный научный журнал)*, Vol. 4, 82-84. <http://dx.doi.org/10.28983/asj.y2019i4pp82-84>
- [15] Li, Y., Zhao, S., Yang, L., Song, Q., Li, B., Yang, F. (2024). Design and Test of High-speed Precision Seeder of Independent Fractionated Soybean Double-row Brush. *Transactions of the Chinese Society for Agricultural Machinery*, Vol. 55(06), pp. 101-110. (in Chinese)
- [16] Noureldin, S., Artyom, D., Andrey, B., Aleksandr, L. (2019). A comparative analysis of precision seed planters. *E3S Web of Conferences*, Vol. 135, 1080. <https://doi.org/10.1051/e3sconf/201913501080>
- [17] Šarauskis, E., Kazlauskas, M., Bručienė, I., Naujokienė, V., Romaneckas, K., Buragienė, S., Steponavičius, D., Abdul Mounem, M. (2023). Impact of soil electrical conductivity-based site-specific seeding and uniform rate seeding methods on winter wheat yield parameters and economic benefits. *Precision Agriculture*, Vol. 24, pp. 2438-2455. <https://doi.org/10.1007/s11119-023-10047-3>
- [18] Sharma, A., Prakash, A., Bhambota, S., Kumar, S. (2024). Investigations of precision agriculture technologies with application to developing countries, *Environment, Development and Sustainability*, Vol. 2024, 18 February. <https://doi.org/10.1007/s10668-024-04572-y>
- [19] Wang, S., Sun, Y., Yang, C., Yu, Y. (2021). Advanced design and tests of a new electrical control seeding system with genetic algorithm fuzzy control strategy. *Journal of Computational Methods in Sciences and Engineering*, Vol. 21(3), pp. 703 -712. <http://dx.doi.org/10.3233/JCM-215126>
- [20] Zhang, B.P. (1997). *Xiandai Zhongzhi Jixie Gongcheng (现代种植机械工程)*. [M], China Machine Press, Beijing. (in Chinese)
- [21] Zhang, F., Qin, C., Wang, X. (2022). Study on leak in seeding prevention and seed protection of disc precision soybean metering device (圆盘精量大豆排种器型孔防空排设计与种子防护研究). *Journal of Agricultural Mechanization Research*, Vol. 44(8), pp. 65-70. DOI: 10.13427/j.cnki.njyi.2022.08.012 (in Chinese)